NIH Public Access
Author Manuscript
J Neurophysiol. Author manuscript; available in PMC 2010 February 23.

Published in final edited form as:
J Neurophysiol. 2005 June ; 93(6): 3649–3658. doi:10.1152/jn.01262.2004.

Prehension Synergies: Trial-to-Trial Variability and Principle of Superposition During Static Prehension in Three Dimensions

Jae Kun Shim, **Mark L. Latash**, and **Vladimir M. Zatsiorsky**
Department of Kinesiology, Penn State University, University Park, Pennsylvania

Abstract

We performed three-dimensional analysis of the conjoint changes of digit forces during prehension (prehension synergies) and tested applicability of the principle of superposition to three-dimensional tasks. Subjects performed 25 trials at statically holding a handle instrumented with six-component force/moment sensors under seven external torque conditions; –0.70, –0.47, –0.23, 0.00, 0.23, 0.47, and 0.70 Nm about a horizontal axis in the plane passing through the centers of all five digit force sensors (the grasp plane). The total weight of the system was always 10.24 N. The trial-to-trial variability of the forces produced by the thumb and the virtual finger (an imagined finger producing the same mechanical effects as all 4 finger forces and moments combined) increased in all three dimensions with the external torque magnitude. The sets of force and moment variables associated with the moment production about the vertical axis in the grasp plane and the axis orthogonal to the grasp plane consisted of two noncorrelated subsets each; one subset of variables was related to the control of grasping forces (*grasp control*) and the other sassociated with the control of the orientation of the hand-held object (*torque control*). The variables associated with the moment production about the horizontal axis in the grasp plane did not include the grip force (the normal thumb and virtual finger forces) and showed more complex noncorrelated subsets. We conclude that the principle of superposition is valid for the prehension in three dimensions. The observed high correlations among forces and moments associated with the control of object orientation could be explained by *chain effects*, the sequences of cause-effect relations necessitated by mechanical constraints.

INTRODUCTION

Multi-finger prehension is performed by a statically redundant system (the hand) that can exert infinite combinations of digit forces and moments to produce a required output. The human CNS, in this sense, confronts a choice of selecting a solution from an apparently infinite set (Bernstein 1935, 1967; Turvey 1990). It has been suggested that the problem of motor redundancy is solved by uniting elemental variables into groups that interact with each other to stabilize task-specific performance variables (d'Avella et al. 2003; Gelfand and Tsetlin 1966; Latash et al. 2002; Scholz and Schoner 1999; Zatsiorsky et al. 2004); such solutions have commonly been addressed as synergies.

One approach to study a synergy in human movement is to examine variability of elemental variables and relations among them over multiple trials for the same motor task. This approach is based on the idea that when more elemental variables contribute to a motor task than absolutely necessary, the CNS does not search for a unique solution but facilitates families of solutions each of which is equally capable of solving the task (Gelfand and Latash 1998; Latash

Copyright © 2005 The American Physiological Society

Address for reprint requests and other correspondence: J. K. Shim, Biomechanics Lab., Dept. of Kinesiology, Rec. Hall-39, The Pennsylvania State University, University Park, PA 16802 (jus149@psu.edu)..

NIH-PA Author Manuscript
NIH-PA Author Manuscript
NIH-PA Author Manuscript

NIH-PA Author Manuscript

NIH-PA Author Manuscript

NIH-PA Author Manuscript

2000). Hence, statistical analysis of the trial-to-trial variability of elemental variables may reveal families of solutions preferred by the CNS for a given motor task (Latash et al. 2001; Schoner 1995; Shim et al. 2003b). The trial-to-trial variability of elemental variables has been studied in a variety of multi-effector systems (Kang et al. 2004; Krishnamoorthy et al. 2003, 2004; Shim et al. 2003a,b, 2004b). In the studies by Shim et al. (2003b) and Zatsiorsky et al. (2004), subjects were asked to hold a customized handle multiple times under the same external load/torque combinations. The task and the analysis were limited to one plane. Patterns of trial-to-trial variability of elemental variables such as digit forces, moments, and moment arms have suggested that the CNS generated families of solutions structured to stabilize the motor performance.

According to the principle of superposition suggested in robotics, some actions can be controlled by independent control processes related to sub-actions (Arimoto et al. 2001; Doulgeri et al. 2002; Parra-Vega et al. 2001). When analyzed in two dimensions (2D), both simulations of a two-digit robot grasping (Arimoto et al. 2002; Nguyen and Arimoto 2002) and experiments with multi-digit human grasping (Shim et al. 2003b; Zatsiorsky et al. 2004) have confirmed the principle of superposition by showing the existence of two subgroups of elemental variables related to *grasp control*—adjustments of the grasping forces—and *torque control*, i.e., the control of rotational equilibrium of the hand-held object.

In this study, we investigated the trial-to-trial variability of elemental variables related to the grasping force and torque production in three dimensions (3D). Based on previous studies (Shim et al. 2003b; Zatsiorsky et al. 2004), we hypothesize that the trial-to-trial variability of resultant finger forces along each axis in 3D increases with the magnitudes of the external torques and the principle of superposition is valid in 3D. This paper is a sequel to previous studies on trial-to-trial variability (Shim et al. 2003b) and the principle of superposition (Zatsiorsky et al. 2004) in 2D quasi-static human prehension tasks.

METHODS

Subjects

Six right-handed males participated in this study as subjects (age: 26.2 ± 2.9 yr, weight: 71.7 ± 3.2 kg, height: 178.8 ± 4.1 cm, hand length: 19.1 ± 2.3 cm, hand width: 8.9 ± 1.1 cm; means ± SD). The hand length was measured between the distal crease of the wrist and the middle fingertip when a subject positioned the palm side of the right hand and the lower arm on a table with all finger joints being extended, and the hand width was measured between the radial side of the index finger metacarpal joint and the ulnar side of the little finger metacarpal joint. The purpose of the study and the involved procedures were explained to the subjects, and all the subjects gave informed consent according to the protocols approved by the Office for Research Protections of the Pennsylvania State University.

Equipment

Five six-component transducers (4 Nano-17s for the fingers and 1 Nano-25 for the thumb, ATI Industrial Automation, Garner, NC) were attached to an aluminum handle to record the forces along three orthogonal axes and the moments about the center of the contact surface about the three axes, Fig. 1*A*.

On the top of the handle, the transmitter of a six-component (3 positions and 3 angles in 3D) magnetic tracking device (Polhemus FASTRAK, Rockwell Collins, Colchester, VT) was installed using a plastic base (0.2 × 17.0 × 13.5 cm); the distance between the transmitter and the receiver was kept within 5 cm. The linearity of the magnetic device was confirmed in the presence of metallic materials around the magnetic device, which potentially could distort the

NIH-PA Author Manuscript

NIH-PA Author Manuscript

NIH-PA Author Manuscript

magnetic field and change the linearity of the signals. In particular, the regression analysis of the 11 independently measured angles versus the angles recorded with the magnetic device yielded the coefficients of determination (r^2) higher than 0.97 about each axis in 3D. An aluminum beam (3.8 × 52.1 × 0.6 cm) was attached to the bottom of the handle; the beam was used to apply external torques to the handle system about *z* axis by hanging a load (0.32 kg) at different positions along the beam. Sandpaper [100-grit; static friction coefficients between the digit tip and the contact surface ranged from 1.4 to 1.5; measured previously (Zatsiorsky et al. 2002)] was placed on the contact surface of each transducer to increase the friction between the digits and the transducers. The sensors were aligned in the *y*-*z* plane. The plane spanned by the *y* and *z* axes will be referred to as the grasp plane. The total weight of the handle, beam, transducers, and suspended load was 10.24 N.

During the experiment, the subjects sat on a chair and positioned their right upper-arm on a wrist-forearm brace that was fixed to the table, Fig. 1*B*. The forearm was held stationary with Velcro straps, and the wrist in the brace was locked in flexion-extension and ulnar deviations. The upper arm was abducted ~45° in the frontal plane and flexed 45° in the sagittal plane. The forearm was aligned parallel to the sagittal axis of the subject. The top of the handle above its center of mass determined without the load was connected to a rack (7.5 × 84.0 × 123.5 cm; not shown in Fig. 1) using a cotton thread. The handle was suspended from the rack ~5 cm below a natural holding position.

Seven different external torques about *z* axis (–0.70, –0.47, –0.23, 0.00, 0.23, 0.47, and 0.70 Nm) were generated by changing the location of the load suspended from the horizontal beam. Before each trial, the experimenter presented the handle in the vertical orientation to the subject. During the trials, the subject grasped the handle at a natural holding position. The subject released the handle after each trial, and the handle was hanging from the rack between trials. Hyperextended joint positions were not allowed for any of the phalangeal joints of the hand. The task and the instructions were designed to achieve a stable trial-to-trial performance: The forearm, wrist, and hand positions were fixed, and the instruction given to the subjects was to hold the handle with the fingertip centers placed at the centers of the sensors and applying a minimal effort. Subjects performed 25 trials for each external torque condition.

The experiments required the subjects to perform several repetitions for each external torque condition. Subjects were instructed to avoid rotating the handle system by watching a cursor on the computer screen, which showed the angular position of the handle about *x* and *z* axes. Angular position about *y* axis was not shown to the subject because handle rotation about *y* axis during a static prehension task does not change the external torque about any of the axes due to the parallel alignment of the line of gravity and *y* axis, but handle rotation about *x* and *z* axes can cause different external torques about *x* and *z* axes. The horizontal and vertical axes passing through the center of the screen corresponded to angular positions of the handle about *x* and *z* axes (θ_x and θ_z), respectively. A circle of 3.0-cm radius was shown at the center of the screen. The radius of the circle represented 1° deviations from the vertical handle orientation. The customized data collection software automatically stopped during experiments when the handle orientation deviated by $>1^\circ$ $\left(1^\circ<\sqrt{\theta_x^2+\theta_z^2}^\circ\right)$. The subjects had 3 s to move the cursor into the circle shown on the computer screen. The data were collected at the sampling frequency of 60 Hz for six seconds and the recorded data were averaged over the second half of the 6-s period in each trial for later analyses.

To avoid fatigue, a minimum 20-s rest interval was given between trials, and a rest interval of 10 min was given between torque conditions. The order of torque conditions was balanced. The subjects performed the tasks successfully. The number of trials in which subjects failed to keep the cursor within the 1° range was 3.6 ± 1.8 (mean ± SD across subjects) trials out of the total 175 trials. The failure trials were not included into analysis.

NIH-PA Author Manuscript

NIH-PA Author Manuscript

NIH-PA Author Manuscript

Data analysis

Because each digit makes a soft-finger contact with the sensor surface (Arimoto et al. 2000; Mason and Salisbury 1985; Shim et al. 2003b), the digit tips can roll on the sensors. Digits could push against the sensors but could not pull on them. The position of the points of digit force application with respect to the center of the surface of the sensor was calculated as $\mathrm{CoP}_x = -(\mathrm{moment})_y/F_z$ and $\mathrm{CoP}_y = (\mathrm{moment})_x/F_z$ [CoP stands for the center of pressure of force along z axis (F_z) on the sensor surface; $(\mathrm{moment})_x$ and $(\mathrm{moment})_y$ signify the moments about x and y axes with respect to the center of the sensor surface]. The moments of force acting on the handle were calculated with respect to the point whose x-y coordinates were the thumb force application point on an x-y plane and the z coordinate of which was located at the center of mass of the handle along z axis.

The data were analyzed at the level of the virtual finger (VF) forces. The VF is an abstract representation of the four individual fingers (IFs); the VF produces the same mechanical effects as all the finger forces and moments combined (Arbib et al. 1985; Baud-Bovy and Soechting 2001; Cutkosky and Howe 1990; MacKenzie and Iberall 1994; Shim et al. 2004a). In other words, the VF force is the vector sum of all IF forces (Eq. 1). The VF produces a free moment on the object as well as the moments of its force. The VF free moment is due to two sources: a VF force couple $\left(m_z^{\mathrm{vf(C)}}\right)$ generated by noncolinear individual finger forces in opposite directions in the x-y plane and a VF twisting moment $\left(m_z^{\mathrm{vf}}\right)$, which is the sum of finger twisting moments $\left(m_z^j\right)$ produced by twisting friction between the finger tips and the contact surfaces (Eq. 2)

$$\overrightarrow{F^{\mathrm{vf}}} = \left[F_x^{\mathrm{vf}}, F_y^{\mathrm{vf}}, F_z^{\mathrm{vf}}\right]^T = \left[\sum_{j=1}^{4} F_x^j, \sum_{j=1}^{4} F_y^j, \sum_{j=1}^{4} F_z^j\right]^T \tag{1}$$

$$m_z^{\mathrm{free}} = m_z^{\mathrm{vf(C)}} + m_z^{\mathrm{vf}} = \sum_{j=1}^{4} M_z^j - M_z^{\mathrm{vf}} + \sum_{j=1}^{4} m_z^j \tag{2}$$

where m_z^{free} is a VF-free moment produced about z axis, M_z^j is the moment of individual finger force about z axis, M_z^{vf} is the moment of the VF force about z axis, and $j = \{\mathrm{index, middle, ring, little}\}$. The VF force was assumed to apply at its CoP calculated as $\mathrm{CoP}_x^{\mathrm{vf}} = -M_y^{\mathrm{vf}}/F_z^{\mathrm{vf}}$ and $\mathrm{CoP}_y^{\mathrm{vf}} = M_x^{\mathrm{vf}}/F_z^{\mathrm{vf}}$. Note that throughout the text small m designates a free moment [a moment of the couple; see (Zatsiorsky 2002, p. 19)] the axis of which can be translated in parallel without a change of the total moment on the handle while capital M identifies the moment about the origin of the global coordinate system shown in Fig. 1. The symbols and definitions of the other elemental variables (the VF and thumb forces and moments) are presented in Fig. 2.

Relations among the variables necessitated by the equilibrium requirements and handle geometry

When the handle is in a static equilibrium, the following equations should be satisfied

NIH-PA Author Manuscript

NIH-PA Author Manuscript

NIH-PA Author Manuscript

$$\overrightarrow{F^{\mathrm{p}}}=\overrightarrow{F^{\mathrm{vf}}}+\overrightarrow{F^{\mathrm{th}}}+\overrightarrow{L}=\left[F_x^{\mathrm{vf}}+F_x^{\mathrm{th}},F_y^{\mathrm{vf}}+F_y^{\mathrm{th}}+L,F_z^{\mathrm{vf}}+F_z^{\mathrm{th}}\right]^T=[0,0,0]^T \tag{3}$$

$$\begin{aligned}\sum_{q=1}^{5}\overrightarrow{M^q}= \quad & \overrightarrow{M^{\mathrm{vf}}}+\overrightarrow{M^{\mathrm{th}}}+\overrightarrow{m^{(\mathrm{C})}}+\overrightarrow{m}+\overrightarrow{\mathrm{Tq}}\\ =\Big[& M_x^{\mathrm{th}(y)}+M_x^{\mathrm{vf}(z)}+M_x^{\mathrm{vf}(y)}M_y^{\mathrm{th}(x)}+M_y^{\mathrm{vf}(x)}+M_y^{\mathrm{vf}(z)}M_z^{\mathrm{vf}(y)}\\ & +M_z^{\mathrm{vf}(x)}+m_z^{\mathrm{vf}(\mathrm{C})}+m_z^{\mathrm{th}}+m_z^{\mathrm{vf}}+\mathrm{Tq}\Big]^T=[0,0,0]^T\end{aligned} \tag{4}$$

where L and Tq, respectively, stand for the weight of the handle and the external torque, superscript T signifies vector transpose, M and m, respectively, represent a moment of force (a moment produced by a force) and a free moment, subscripts x, y, and z signify the moment axes, and the superscript vf and th stand for the virtual finger and the thumb, respectively. The horizontal arrows above the symbols signify vectors.

While all the individual force and moments are voluntarily controlled, perfect or close to perfect coefficients of correlation are expected between the variables when the geometry of the handle and/or the equations of static equilibrium require this (Fig. 3). An immediate reason behind such high correlations may be not trivial; it may involve multi-step sequences of the cause-effect relations among the variables, so called *chain effects* (Shim et al. 2004a;Zatsiorsky et al. 2004). For instance, an observed high correlation between the VF vertical force $\left(F_y^{\mathrm{vf}}\right)$ and the moment about anterior-posterior axis x generated by the VF horizontal normal force $M_x^{\mathrm{vf}(z)}$ (Fig. 3, panel X–IV) can be explain by the following chain effects: *1*) the perfect correlations ($r = 1.00$) between the VF vertical tangential force $\left(F_y^{\mathrm{th}}\right)$ and the moment of VF vertical tangential force $\left(M_x^{\mathrm{vf}(y)}\right)$ in the panel X–I are expected because the moment is simply a product of the force and the constant moment arm $\left(M_x^{\mathrm{vf}(y)}=F_y^{\mathrm{vf}}\cdot W/2\right)$. *2*) The moment of vertical VF force about the anterior-posterior x axis $m_x^{\mathrm{vf}(y)}$ highly correlates with the moment generated by the thumb vertical tangential force $\left(M_x^{\mathrm{th}(y)}\right)$ due to the existing constraints $F_y^{\mathrm{th}}+F_y^{\mathrm{vf}}\ L$ and $-d_z^{\mathrm{th}}=d_z^{\mathrm{vf}}$. *3*) The total moment about x axis is the sum of the three moments $\left(M_x=M_x^{\mathrm{vf}(y)}+M_x^{\mathrm{th}(y)}+M_z^{\mathrm{vf}(z)}\right)$. Because the positive correlation between $M_x^{\mathrm{vf}(y)}$ and $M_x^{\mathrm{th}(y)}$ is necessitated by the equations in *2* and the task includes maintaining a constant M_x, the correlations between $M_x^{\mathrm{th}(y)}$ and $M_x^{\mathrm{vf}(z)}$ as well as between $M_x^{\mathrm{vf}(y)}$ and $M_x^{\mathrm{th}(y)}$ should be negative. High negative correlations between $M_x^{\mathrm{th}(y)}$ and $M_x^{\mathrm{vf}(z)}$ are shown in X–III. *4*) The relation between F_y^{vf} and $M_x^{\mathrm{vf}(z)}$ in X-IV is necessitated by the aforementioned relations (X–I, X–II, and X–III), or in other words, it is necessitated by the task geometry and task mechanics.

A similar explanation can be employed to explicate the variables relations in M_y group, Fig. 3*Y*.

Statistics

Regression analysis was performed between elemental variables, and Pearson's coefficients of correlation (r) were calculated and corrected for noise and error propagations (see Shim et al. 2003b for computational details) in MATLAB. The significance level was set at $P < 0.05$. For $n = 25$, the border value of the correlation coefficient is $r = 0.40$ for a linear regression; for n

NIH-PA Author Manuscript

NIH-PA Author Manuscript

NIH-PA Author Manuscript

= 7, the border value of the correlation coefficient is $r = 0.75$ for a linear regression and $r = 0.81$ for a quadratic regression, respectively.

For each external torque condition, sets of elemental variables related to moment production were grouped for each axis (M_x group: $F_z^{vf}, F_z^{th}, M_x^{vf(y)}, M_x^{vf(z)}$, and $M_x^{th(y)}$; M_y group: $F_z^{vf}, F_z^{th}, M_y^{vf(z)}, M_y^{vf(x)}$, and $M_y^{th(x)}$; M_z group: $F_z^{vf}, F_y^{vf}, m_z^{vf}, m_z^{th}, m_z^{(C)}, M_z^{vf(x)}$, and $M_z^{vf(y)}$). Note that in the groups we included the variables that are coupled by equilibrium constraints, but require the CNS control (e.g., both F_z^{vf} and F_z^{th} are included in M_x group), while we did not include the variables that are coupled by the handle geometry (e.g., $M_x^{vf(y)}$ was included in M_x group but F_y^{th} was not because $M_x^{vf(y)}$ equals a product of F_y^{th} and a constant moment arm, a half of grip width of the handle). The corrected correlations between the elemental variables in each group were used to construct a correlation matrix. As an estimate of communality (elements of the main diagonal of a correlation matrix), the values of 1.0 were used. This matrix was used to perform a principal components analysis (PCA) with a variance maximizing (varimax) rotation in MATLAB. The eigenvectors with eigenvalues >1 (Kaiser Criterion) (Kaiser 1960) were extracted as principal components (PCs) and the loading coefficients for each variable were calculated in the PCs. A customary cutoff loading coefficient of 0.4 was used as a minimal significant loading value.

RESULTS

Force-force relations at VF level in 3D

The VF and thumb forces along each axis showed high significant negative correlations for all external torque conditions in all subjects (Fig. 4). Such mechanically necessitated correlations were expected from Eq. 3.

Trial-to-trial variability of force in 3D

The trial-to-trial variability of VF and thumb forces along x and z axes ($F_x^{vf}, F_x^{th}, F_z^{vf}$, and F_z^{th}), expressed as the SD computed across trials, increased with the force magnitude (X–I and Z–I in Fig. 5). The variability of F_y^{vf} and F_y^{th} was small when the force magnitudes were close to the half of the handle's weight (10.24 N), and the variability increased when the magnitudes of the forces deviated from this value (Y–I in Fig. 5). Along each axis, the indices of force variability of the VF and thumb showed very high correlations (X–II, Y–II, and Z–II in Fig. 5). Note that the intercepts of the regression equations are 0 and the slopes are 1. The variability of the VF and thumb forces along each axis increased with the external torque magnitude (X–III, Y–III, and Z–III in Fig. 5). For each subject, the coefficients of correlation shown in Fig. 5 were all significant except the coefficients of correlation in the panel X–I: r {–0.88, –0.33} for F_x^{vf} and $r = \{0.49, 8.10\}$ for F_x^{th} (ranges of coefficients of correlation are reported across all external torque conditions in each subject).

Correlation between forces and moments produced by these forces

As expected, the perfect relations ($|r| = 1$) between the forces and the moments produced by them were found between forces and moments of the forces the moment arms of which were constant. However, when moment arms could vary along x or y axis—due to variation in the individual finger positions with respect to the sensor centers and/or variation in individual finger force shares—the coefficients of correlation between the forces and the moments that these forces produce become very low (pairs of variables F_z^{vf} vs. $M_x^{vf(z)}$: $r = \{0.04, 0.31\}$, F_z^{vf} vs. $M_y^{vf(z)}$: $r = \{-0.01, 0.12\}$, F_x^{vf} vs. $M_z^{vf(x)}$: $r = \{-0.36, 0.41\}$, F_y^{vf} vs. $M_z^{vf(y)}$: $r = \{-0.25, 0.07\}$;

NIH-PA Author Manuscript

NIH-PA Author Manuscript

NIH-PA Author Manuscript

ranges of coefficients of correlation are reported across all external torque conditions in each subject).

Inter-relations of forces and moments associated with moment production about coordinate axes

Principal component analysis (PCA) of elemental variables associated with the moment production about individual coordinate axes showed considerable differences between z axis and x and y axes. The elemental variables associated with the moment production about x axis (M_x group) and the variables related to the moment production about y axis (M_y group) showed two noncorrelated subsets: the first subset was related to the control of stable grasping, i.e., grasping the object weaker or stronger (*grasp control*), and the other subset was associated with the control of torque exerted on the handle, i.e., control of the orientation of the handle about x or y axis (*torque control*). In contrast, the elemental variables contributing to the moment production about z axis (M_z group) did not show meaningful grouping into individual subsets.

PCA on M_x group variables

The elemental variables associated with the moment production about x axis (M_x group) are: F_z^{vf}, F_z^{th}, $M_x^{vf(y)}$, $M_x^{vf(z)}$, and $M_x^{th(y)}$. F_y^{vf} and F_y^{th} were not included in M_x group because they had perfect coefficients of correlation ($|r| = 1.0$), respectively, with $M_x^{vf(y)}$ and $M_x^{th(y)}$ due to the task constraints $M_x^{vf(y)} = F_z^{vf} \cdot W/2$ and $M_x^{th(y)} = -F^{y}th \cdot W/2$, where W is the grip width. $M_x^{th(z)}$ was also not included because all moments of forces were calculated with respect to the thumb force application point; see METHODS for details. The PCA revealed two PC_s ($PC1_X$ and $PC2_X$) that accounted for 98.54 ± 0.50% of the total variance (average ± SD across external torque conditions after the results were averaged across the subjects for each external torque condition).

The loadings for each elemental variable were calculated for $PC1_X$ and $PC2_X$, Table 1. The moment variables ($M_x^{vf(y)}$, $M_x^{vf(z)}$, and $M_x^{th(y)}$) had large loading magnitudes in $PC1_X$, but small loadings in $PC2_X$. VF and thumb normal forces (F_z^{vf} and F_z^{th}) showed large loadings in $PC2_X$ but small loadings in $PC1_X$. Regression analysis showed that the variables that had high loadings in the same PC had coefficients of correlation (r) close to perfect ($|r| > 0.90$) between each other, but nonsignificant coefficients of correlation ($|r| < 0.40$) with the variables in the other PC. These findings were true for all external torque conditions in each subject. The signs of the loadings were mechanically necessitated by the requirement of static equilibrium.

PCA on M_y group variables

The elemental variables associated with the moment production about y axis (M_y group) are: F_z^{vf}, F_z^{th}, $M_y^{vf(z)}$, $M_y^{vf(x)}$, and $M_y^{th(x)}$. F_x^{vf}, F_x^{th}, and $M_y^{th(z)}$ were not included in M_y group due to the reasons similar to the explained in the preceding text for the M_x group.

Two PCs ($PC1_Y$ and $PC2_Y$) accounted for 96.81 ± 1.81% of the total variance (average ± SD across external torque conditions after the results were averaged across the subjects for each external torque condition). The structure of the loadings of M_y group variables was similar to that of M_x group variables, Table 2. The large loadings of the moment variables ($M_x^{vf(z)}$, $M_y^{vf(x)}$, and $M_y^{th(x)}$) were found in $PC1_Y$ and the large loadings of VF and thumb normal forces (F_z^{vf} and F_z^{th}) were observed in $PC2_Y$. The variables with high loadings in the same PC had coefficients of correlation (r) close to perfect ($|r| > 0.91$) between each other but insignificant coefficients of correlation ($|r| < 0.40$) with the variables in the other PC. This was

NIH-PA Author Manuscript

NIH-PA Author Manuscript

NIH-PA Author Manuscript

true for all external torque conditions in each subject. The signs of the loadings were mechanically necessitated by the requirement of static equilibrium.

PCA on M_z group variables

Elemental variables associated with the moment production about z axis (M_z group) are: $F_x^{vf}, F_y^{th}, m_z^{vf}, m_z^{th}, m_z^{(C)}, M_z^{vf(x)}$, and $M_z^{vf(y)}$. Note that the grip forces (F_z^{vf} and F_z^{th}) were not included in M_z group because changes of the grip forces do not affect output of M_z. Kaiser criterion generated three PCs that accounted for 92.90 ± 0.23% of the total variance (across external torque conditions after the results were averaged across the subjects for each external torque condition), Table 3. However, on two PCs out of three there were only one variable with large loading. Hence, the PCA failed in separating the entire set of variables into two or a few subsets with the large correlations in individual subsets. This was true for all external torque conditions in each subject. This finding does not contradict the principle of superposition according to which the grip force and the torque are controlled as separate entities because the grip forces, F_z^{vf} and F_z^{th}, were not included in the present analysis.

Inter-relations among all elemental variables (M_{3D})

We also performed PCAs on all 13 variables for each external torque condition. Kaiser criterion generated three PCs ($PC1_{3D}$ to $PC3_{3D}$) which accounted for 94.80 ± 0.65% of the total variance (across external torque conditions after the results were averaged across the subjects for each external torque condition), Table 4. Among the three PCs, one PC had large loadings (absolute values >0.95) of VF and thumb grasping forces (F_z^{vf} and F_z^{th}). Two other PCs had large loadings (absolute values >0.86) on the sets of elemental variables associated with the moments about x and y axes, respectively. These findings were true for all external torque conditions in each subject. This finding is in agreement with the principle of superposition. Other elemental variables did not load significantly on the first three PCs generated by the Kaiser Criterion. These results were true for each external torque conditions and each subject.

DISCUSSION

In this study, the trial-to-trial variability of elemental variables during a 3D static grasping was investigated, and several hypotheses were tested related to the principle of superposition and dependencies of VF finger force variability on the force and external torque magnitude. The trial-to-trial variability of the VF and thumb forces along each axis increased with the external torque magnitude. The PCA clearly separated elemental variables into two subsets for both M_x and M_y groups: the VF and thumb grasping forces and the variables immediately contributing to the moment production. In M_{3D} group, grasping forces were decoupled from other variables. Hence, the principle of superposition was generally supported for 3D prehension.

The DISCUSSION addresses the following topics: variability of VF and thumb forces in 3D, chain effects as an explanation for high correlations between some of the variables, relations between forces and moments of the forces as an explanation of noncorrelated subsets of variables, relations among the elemental moment variables in M_z, and principle of superposition in 3D.

Variability of forces

The variability of VF and thumb forces increased with force magnitude as well as with external torque, as it could be expected from many earlier studies on finger force variability during pressing and prehension (Newell and Carlton 1988; Newell et al. 1984; Pataky et al. 2004; Shim et al. 2003b, 2004b). The variability of VF and thumb vertical forces (F_y^{vf} and F_y^{th}) had

NIH-PA Author Manuscript

NIH-PA Author Manuscript

NIH-PA Author Manuscript

a minimum when the force magnitudes were close to each other. This phenomenon has been reported for a 2D prehension task (Shim et al. 2003b) in which V-shaped relations were reported between F_y^{vf} and F_y^{th} and their indices of variability. In the mentioned study (Shim et al. 2003b), the subjects produced positive or negative force along *y* axis depending on the direction of the external torque about *x* axis. In the current study, the subjects did not produce negative F_y^{vf} and F_y^{th}, thus revealing only the left or the right branches of the V-shape relation for the VF and thumb forces, respectively.

The variability of the VF and the thumb forces in all three directions changed identically with $r = 1.0$ (X–II, Y–II, and Z–II in Fig. 5). Such a perfect correlation is necessitated by the task mechanics: the VF and thumb forces in each direction should satisfy the equilibrium constraint (Eq. 3). Consequently, an increase/decrease in one force should be associated with the increase/decrease in the other force. As a result, the increased variability of one force was always associated with increased variability of the other force.

Relations among the variables

relations among the forces and moments produced by these forces. In the present study, the coefficients of correlation between the forces and the moments produced by the same forces were either perfect ($|r| = 1$) when the moment arm was constant or statistically not significant when the moment arm could vary. The latter resulted in noncorrelated subsets of variables in PCA analyses. Under the noncorrelated subsets of variables, we imply splitting them into subgroups with a high correlation between the variables within a subgroup and close to zero correlation among the variables from different subgroups. Having a moment arm, which could vary due to the rolling of the digits or the different sharing of digit forces resulted in very low correlations between the force and the moment. This suggests that the CNS controls the grasping force and its moment arms as two independent entities. Such a claim is essentially equivalent to the principle of superposition.

Relation among the elemental moment variables in M_z

All subjects showed significant negative correlations ($r = \{-0.70, -0.49\}$; ranges of coefficients of correlation are reported) between the VF force couple about *z* axis $\left(m_z^{vf(C)}\right)$ and the thumb twisting moment about *z* axis $\left(m_z^{th}\right)$ for all external torque conditions, reflected in opposite signs of loading coefficients for m_z^{th} and $m_z^{vf(C)}$ in $PC1_Z$, Table 4. Because the thumb is not capable of producing an active twisting moment, m_z^{th}, this relation partially reflects the passive reaction moment of the pad of the thumb tip to $m_z^{(C)}$. In a simple model where the contact area of the thumb is circular and the pressure is evenly distributed over the contact area with a radius (*r*), the relation between the twisting moment of the thumb $\left(m_z^{th}\right)$ and the VF couple about *z* axis $\left(m_z^{vf(C)}\right)$ is

$$m_z^{th} + m_z^{vf(C)} + m_z^{vf} + M_z^{vf(x)} + M_z^{vf(y)} = -\mathrm{Tq} \quad (5)$$

Assume a constant external torque Tq. $M_z^{vf(y)}$ is very small and produces only 0.4% of the total moment about z axis, M_z due to the short moment arm (Shim et al. 2004a); $m_z^{vf(C)}$ (65% of M_z) and $M_z^{vf(x)}$ (25% of M_z) showed negative correlations with each other, but they were not perfectly compensated ($r = \{-0.76, 0.30\}$; ranges of coefficients of correlation are reported

NIH-PA Author Manuscript

NIH-PA Author Manuscript

NIH-PA Author Manuscript

across all external torque conditions in each subject). Hence $m_z^{\mathrm{vf(C)}}$ was further compensated by m_z^{th}.

Principle of superposition in 3D

Considering the results from the PCAs and regression analyses, we have concluded that the variables within the M_x group were decoupled into two subsets as previously found in 2D prehension studies in both robotics (Arimoto and Nguyen 2001; Arimoto et al. 2001, 2003) and human motor control (Shim et al. 2003b; Zatsiorsky et al. 2004). One subset of variables (F_z^{vf} and F_z^{th}) was related to grasp control, i.e., grasping an object weaker or stronger, which has been a favorite topic in human prehension studies (Augurelle et al. 2003; Cole and Abbs 1988; Gilles and Wing 2003; Johansson and Westling 1988; Turrell et al. 1999). The other subset of variables was associated with torque control, i.e., control of the orientation of a hand-held object about *x* axis, which has relatively recently drawn attention from researchers (Kinoshita et al. 1997; Santello and Soechting 2000; Shim et al. 2004b; Zatsiorsky et al. 2003). The variables of M_y group were also decoupled into two subsets of variables; the first subset had the same variables as in M_x group (F_z^{vf} and F_z^{th}; the variables of grasp control) and the second subset contained the variables of torque control about *y* axis. The conjoint changes or synergies of grasp control variables prevent a hand-held object from slipping out of the hand and linear translation of the object along *z* axis. The conjoint variations of torque control variables avoid the change in orientation of the hand-held object as well as the translation of the hand-held object along *x* axis for M_y or *y* axis for M_x. The decoupled subsets of variables support the principle of superposition in human prehension in M_x group and M_y group.

PCA failed to clearly decompose M_z group variables into meaningful subsets. Only one subset comprised more than one variable, a moment of a couple $\left(m_z^{(\mathrm{C})}\right)$ and a moment of F_x^{vf}, which showed negative coefficients of correlations reflected in the opposite signs in the loading coefficients in Table 4. The negative correlations were mechanically necessitated because a larger finger tangential force producing $m_z^{(\mathrm{C})}$ is associated with a smaller tangential force generating $M_z^{\mathrm{vf}(x)}$ (see *Eq. 9* in (Shim et al. 2004a) for details).

Within the $M_{3\mathrm{D}}$ group, the grasp control variables (F_z^{vf} and F_z^{th}) were decoupled in the group: the grasping control (the slipping prevention) is realized separately from other subtasks that have to be solved by the CNS during prehension, e.g., maintaining the rotational equilibrium of the object (the word "separately" is used here with the meaning that the changes of the grasping forces F_z^{vf} and F_z^{th} while being perfectly matched to each other do not immediately affect other elemental variables). Elemental moment variables about axes *x* and *y* were also decoupled. Therefore we can conclude that the principle of superposition is valid in a 3D static prehension.

The grouping of elemental variables into a few subsets related to stabilization of different performance variables is a relatively novel observation. Earlier studies of force production in four-finger pressing tasks have shown that humans can stabilize a value of the total force and a value of the total pronation/supination moment at the same time (Latash et al. 2001, 2002; Scholz et al. 2002). However, no clear grouping of the finger forces has been reported that would suggest formation of two finger subgroups related to each of the performance variables separately. During multi-finger quick force pulse production, the peak and the timing of the total force are both defined by a rather complex interaction between the peaks and the timings of the individual finger force pulses. In an earlier study (Latash et al. 2004), PCA revealed a strong coupling among finger peak force values that stabilized the total peak force. There was also strong positive correlation among the timings of individual force peaks. However, PCA

NIH-PA Author Manuscript

NIH-PA Author Manuscript

NIH-PA Author Manuscript

showed no PCs that would contain significantly loaded both magnitude and timing variables i.e., it suggested decoupled control of the timing and of the magnitude of the total force peak.

Our previous study of the principle of superposition in 2D prehension (Zatsiorsky et al. 2004) suggested two aspects of principle of superposition in human prehension. One was grouping of elemental mechanical variables into grasp control and torque control, and the other dealt with the superposition of two commands related to the control of the resultant force acting on a hand-held object and the torque generated on the object, respectively. The second aspect of the principle of superposition in 3D prehension requires further investigation because the loading of the handle was not varied in the present study.

Acknowledgments

This study was supported in part by National Institutes of Health Grants AG-018751, AR-048563, M01 RR-10732, and NS-35032.

REFERENCES

Arbib, MA.; Iberall, T.; Lyons, D. Coordinated control programs for movements of the hand.. In: Goodwin, AW.; Darian-Smith, I., editors. Hand Function and the Neocortex. Springer-Verlag; Berlin: 1985. p. 111-129.*Exp Brain Res Suppl* 10

Arimoto S, Doulgeri Z, Nguyen PTA, Fasoulas J. Stable pinching by a pair of robot fingers with soft tips under the effect of gravity. Robotica 2002;20:241–249.

Arimoto S, Nguyen PTA. Principle of superposition for realising dexterous pinching motions of a pair of robot fingers with soft-tips. IEICE Trans Fund Electr Commun Comp Sci E 2001;84A:39–47.

Arimoto S, Nguyen PTA, Han HY, Doulgeri Z. Dynamics and control of a set of dual fingers with soft tips. Robotica 2000;18:71–80.

Arimoto S, Tahara K, Bae JH, Yoshida M. A stability theory of a manifold: concurrent realization of grasp and orientation control of an object by a pair of robot fingers. Robotica 2003;21:163–178.

Arimoto S, Tahara K, Yamaguchi M, Nguyen PTA, Han HY. Principles of superposition for controlling pinch motions by means of robot fingers with soft tips. Robotica 2001;19:21–28.

Augurelle AS, Penta M, White O, Thonnard JL. The effects of a change in gravity on the dynamics of prehension. Exp Brain Res 2003;148:533–540. [PubMed: 12582839]

Baud-Bovy G, Soechting JF. Two virtual fingers in the control of the tripod grasp. J Neurophysiol 2001;86:604–615. [PubMed: 11495936]

Bernstein NA. The problem of interrelation between coordination and localization (in Russian). Arch Biol Sci 1935;38:1–35.

Bernstein, NA. The Co-ordination and Regulation of Movements. Pergamon; Oxford: 1967.

Cole KJ, Abbs JH. Grip force adjustments evoked by load force perturbations of a grasped object. J Neurophysiol 1988;60:1513–1522. [PubMed: 3193168]

Cutkosky, MR.; Howe, RD. Dextrous Robot Hands. Springer Verlag; New York: 1990.

d'Avella A, Saltiel P, Bizzi E. Combinations of muscle synergies in the construction of a natural motor behavior. Nat Neurosci 2003;6:300–308. [PubMed: 12563264]

Doulgeri Z, Fasoulas J, Arimoto S. Feedback control for object manipulation by a pair of soft tip fingers. Robotica 2002;20:1–11.

Gelfand IM, Latash ML. On the problem of adequate language in movement science. Mot Control 1998;2:306–313.

Gelfand, IM.; Tsetlin, M. On mathematical modeling of the mechanisms of the central nervous system.. In: Gelfand, IM.; Gurfinkel, VS.; Fomin, SV.; Tsetlin, ML., editors. Models of the Structural-Functional Organization of Certain Biological Systems. Nauka; Moscow: 1966. p. 9-26. (a translation is available in 1971 edition by MIT Press: Cambridge, MA)

Gilles MA, Wing AM. Age-related changes in grip force and dynamics of hand movement. J Mot Behav 2003;35:79–85. [PubMed: 12724101]

NIH-PA Author Manuscript

NIH-PA Author Manuscript

NIH-PA Author Manuscript

Johansson RS, Westling G. Coordinated isometric muscle commands adequately and erroneously programmed for the weight during lifting task with precision grip. Exp Brain Res 1988;71:59–71. [PubMed: 3416958]

Kaiser HF. The application of electronic computers to factor analysis. Ed. Psychol. Meas 1960;20:141–151.

Kang N, Shinohara M, Zatsiorsky VM, Latash ML. Learning multi-finger synergies: an uncontrolled manifold analysis. Exp Brain Res. 2004

Kinoshita H, Backstrom L, Flanagan JR, Johansson RS. Tangential torque effects on the control of grip forces when holding objects with a precision grip. J Neurophysiol 1997;78:1619–1630. [PubMed: 9310447]

Krishnamoorthy V, Latash ML, Scholz JP, Zatsiorsky VM. Muscle synergies during shifts of the center of pressure by standing persons. Exp Brain Res 2003;152:281–292. [PubMed: 12904934]

Krishnamoorthy V, Latash ML, Scholz JP, Zatsiorsky VM. Muscle modes during shifts of the center of pressure by standing persons: effect of instability and additional support. Exp Brain Res 2004;157:18–31. [PubMed: 14985897]

Latash ML. There is no motor redundancy in human movements. There is motor abundance. Mot Control 2000;4:259–260.

Latash ML, Scholz JF, Danion F, Schoner G. Structure of motor variability in marginally redundant multifinger force production tasks. Exp Brain Res 2001;141:153–165. [PubMed: 11713627]

Latash ML, Scholz JP, Schoner G. Motor control strategies revealed in the structure of motor variability. Exerc Sport Sci Rev 2002;30:26–31. [PubMed: 11800496]

Latash ML, Shim JK, Zatsiorsky VM. Is there a timing synergy during multi-finger production of quick force pulses? Exp Brain Res 2004;159:65–71. [PubMed: 15480588]

MacKenzie, CL.; Iberall, T. The Grasping Hand. Elsvier Science; Amsterdam: 1994.

Mason, MT.; Salisbury, KJ. Robot Hands and the Mechanics of Manipulation (Artificial Intelligence). MIT Press; Cambridge, MA: 1985.

Newell KM, Carlton LG. Force variability in isometric tasks. J Exp Psychol Hum Percept Performe 1988;14:32–44.

Newell KM, Carlton LG, Hancock PA. Kinetic analysis of response variability. Psychol Bull 1984;96:133–151.

Nguyen PTA, Arimoto S. Computer simulation of controlled motion of dual fingers with soft tips grasping and manipulating an object. Adv Robotics 2002;16:123–145.

Parra-ega V, Rodriguez-Angeles A, Arimoto S, Hirzinger G. High precision constrained grasping with cooperative adaptive handcontrol. J Intell Robotic Syst 2001;32:235–254.

Pataky T, Latash M, Zatsiorsky V. Tangential load sharing among fingers during prehension. Ergonomics 2004;47:876–889. [PubMed: 15204280]

Santello M, Soechting JF. Force synergies for multifingered grasping. Exp Brain Res 2000;133:457–467. [PubMed: 10985681]

Scholz JP, Danion F, Latash ML, Schoner G. Understanding finger coordination through analysis of the structure of force variability. Biol Cybern 2002;86:29–39. [PubMed: 11918210]

Scholz JP, Schoner G. The uncontrolled manifold concept: identifying control variables for a functional task. Exp Brain Res 1999;126:289–306. [PubMed: 10382616]

Schoner G. Recent developments and problems in human movement science and their conceptual implications. Ecol Psychol 1995;8:291–314.

Shim JK, Latash ML, Zatsiorsky VM. The human central nervous system needs time to organize task-specific covariation of finger forces. Neurosci Lett 2003a;353:72–74. [PubMed: 14642441]

Shim JK, Latash ML, Zatsiorsky VM. Prehension synergies: trial-to-trial variability and hierarchical organization of stable performance. Exp Brain Res 2003b;152:173–184. [PubMed: 12898101]

Shim JK, Latash ML, Zatsiorsky VM. Prehension synergies in three dimensions. J Neurophysiol 2004a; 93:766–776. [PubMed: 15456799]

Shim JK, Lay BS, Zatsiorsky VM, Latash ML. Age-related changes in finger coordination in static prehension tasks. J Appl Physiol 2004b;97:213–224. [PubMed: 15003998]

NIH-PA Author Manuscript

NIH-PA Author Manuscript

NIH-PA Author Manuscript

Turrell YN, Li FX, Wing AM. Grip force dynamics in the approach to a collision. Exp Brain Res 1999;128:86–91. [PubMed: 10473745]

Turvey MT. Coordination. Am Psychol 1990;45:938–953. [PubMed: 2221565]

Zatsiorsky, VM. Kinetics of Human Motion. Human Kinetics; Champaign, IL: 2002.

Zatsiorsky VM, Gao F, Latash ML. Prehension synergies: effects of object geometry and prescribed torques. Exp Brain Res 2003;148:77–87. [PubMed: 12478398]

Zatsiorsky VM, Gregory RW, Latash ML. Force and torque production in static multifinger prehension: biomechanics and control. I. Biomechanics. Biol Cybern 2002;87:50–57. [PubMed: 12111268]

Zatsiorsky VM, Latash ML, Gao F, Shim JK. The principle of superposition in human prehension. Robotica 2004;22:231–234.

NIH-PA Author Manuscript

NIH-PA Author Manuscript

NIH-PA Author Manuscript

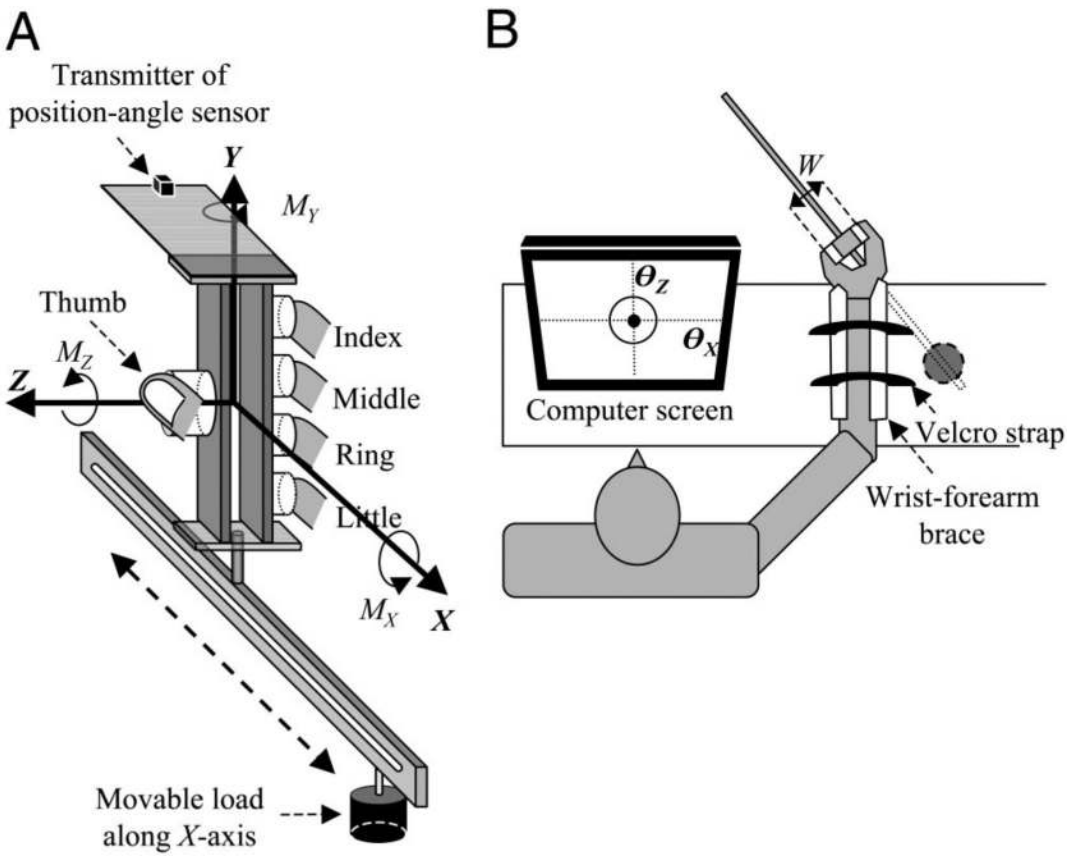

FIG. 1.

A: the customized handle; the force-moment sensors shown as white cylinders were attached to 2 vertical aluminum bars, and a movable load shown as the black cylinder was attached to the long horizontal aluminum beam. The transmitter of a magnetic position-angle sensor shown as a small black cube was attached to the plastic base affixed to the top of the handle. M_x, M_y, and M_z are the moments produced by digits with respect to the *x*, *y*, and *z* axes, respectively. *B*: the subject held the handle while monitoring its angular position about *x* and *z* axes, θ_x and θ_z, respectively. The wrist and the forearm are housed in a wrist-forearm brace and secured with a Velcro strap. W, grip width.

NIH-PA Author Manuscript
NIH-PA Author Manuscript
NIH-PA Author Manuscript

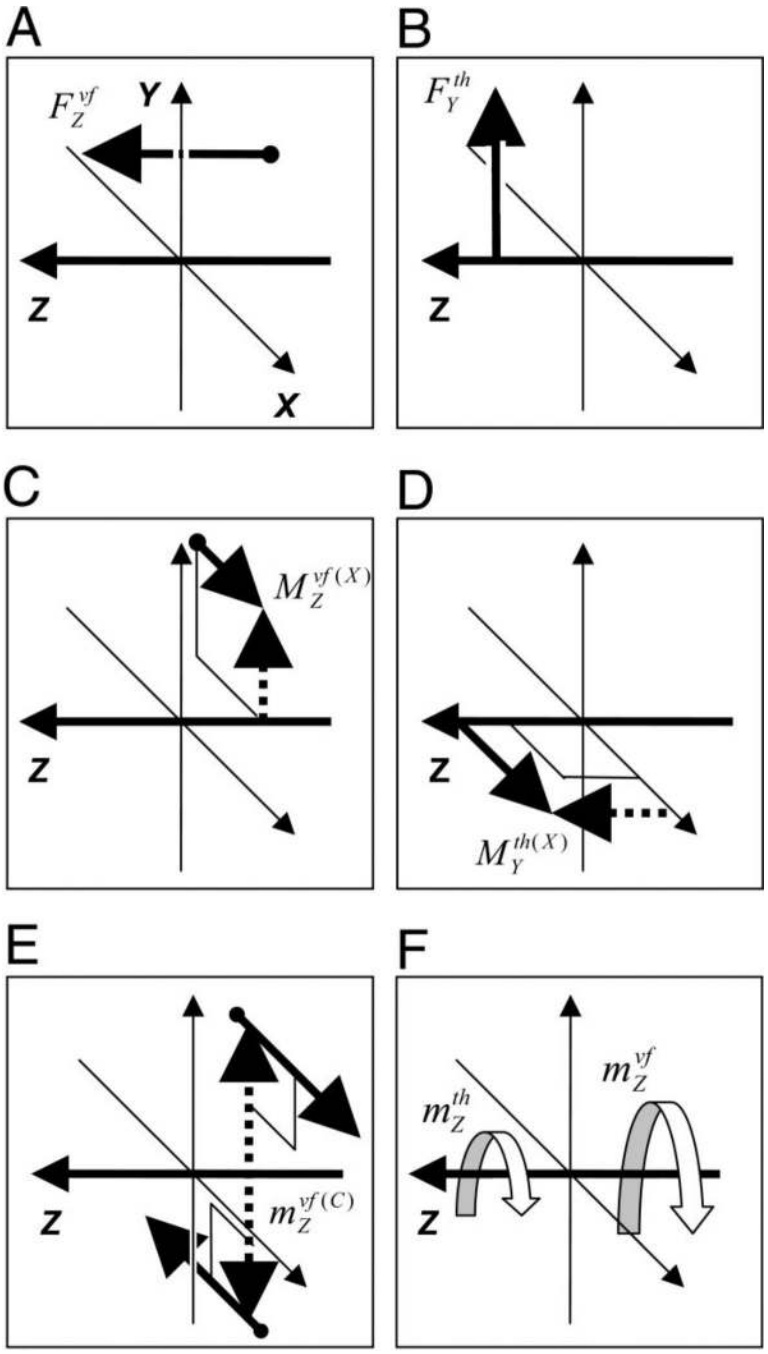

FIG. 2.

Definitions of forces and moments of the virtual finger (VF) and thumb. *A*: VF force along *z* axis $\left(F_z^{\mathrm{vf}}\right)$. *B*: thumb force along *y* axis $\left(F_y^{\mathrm{th}}\right)$. *C*: moment of F_x^{vf} about *z* axis $\left(M_z^{\mathrm{vf(C)}}\right)$. *D*: moment of F_x^{th} about *y* axis $\left(M_y^{\mathrm{th}(x)}\right)$. *E*: VF force couple about *z* axis $\left(m_z^{\mathrm{vf(C)}}\right)$. *F*: VF and thumb twisting moment about *z* axis (m_z^{vf} and m_z^{th}). Similar nomenclatures are applied to the other axes. Line arrows are the forces and dotted arrows are moment arms.

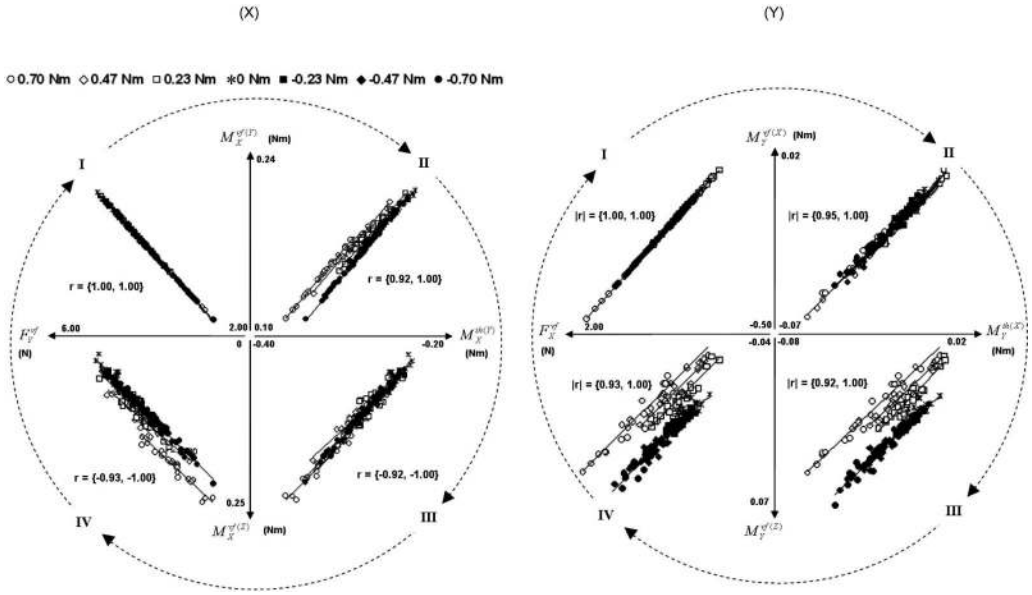

FIG. 3.

Interrelations among the variables contributing to M_x (set of panels X) and M_y (set of panels Y). The graphs should be read in the sequence indicated by the arrows. Panels X: (X–I) F_y^{vf} vs. $M_x^{vf(y)}$, (X–II) $M_x^{vf(y)}$ vs. $M_x^{th(y)}$, (X–III) $M_x^{th(y)}$ vs. $M_x^{th(z)}$, (X–IV) $M_x^{vf(z)}$ vs. F_y^{vf}. Panels Y: (Y–I) F_y^{vf} vs. $M_y^{vf(x)}$, (Y–II) $M_y^{vf(x)}$ vs. $M_y^{th(x)}$, (Y–III) $M_y^{th(x)}$ vs. $M_y^{vf(z)}$, and (Y–IV) $M_y^{vf(z)}$ vs. F_x^{vf}. The ranges of the coefficients of correlation corrected for noise and error propagations are presented in curly braces. Data are from 7 external torque conditions in a representative subject. Smaller values are aligned at the center for both panels X and Y. The different regression lines between pairs of variables for different torque values (such as in X–IV) are probably due to slightly different location of the fingertips on the sensors in these tasks or slightly different orientations of the handle for each external torque conditions [e.g., average angular positions of the handle about Z axis varied from –0.08 ± 0.05° (mean ± SD across trials) to 0.03 ± 0.04° for different external torque values].

NIH-PA Author Manuscript NIH-PA Author Manuscript NIH-PA Author Manuscript

NIH-PA Author Manuscript

NIH-PA Author Manuscript

NIH-PA Author Manuscript

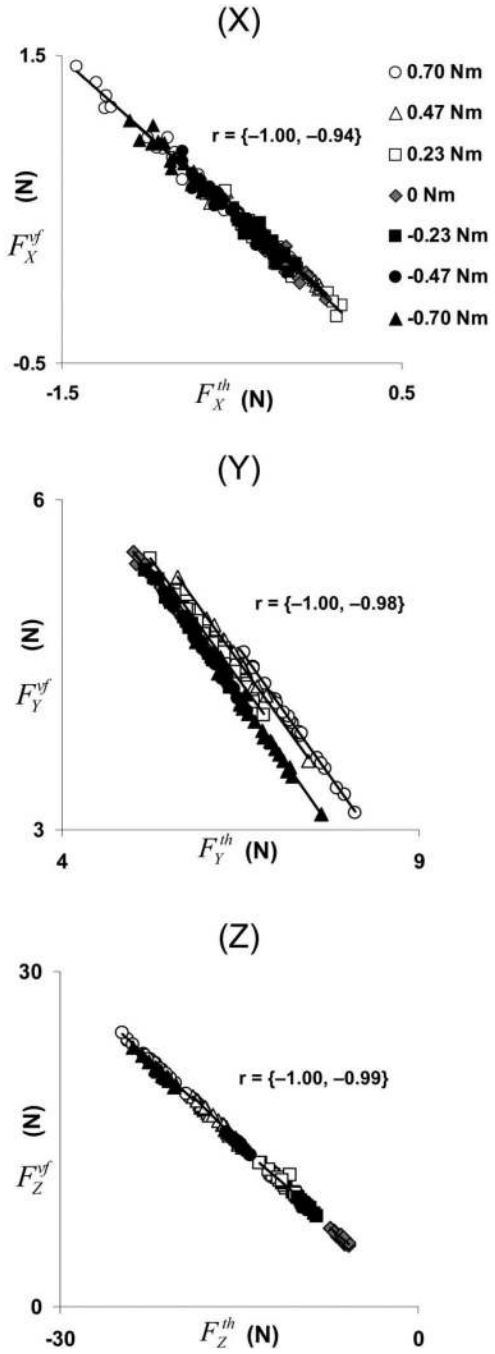

FIG. 4.

Relations between the VF and thumb forces recorded in individual trials. (*X*) F_x^{vf} vs. F_x^{th}, *Y* F_y^{vf} vs. F_y^{th}, and (*Z*) F_z^{vf} vs. F_z^{th}. The ranges of the coefficients of correlation (*r*) over the 7 external torque conditions are presented in curly braces. Data are from a representative subject.

Note that the negative correlations of the grasping forces (F_z^{vf} vs. F_z^{th}) are due to the opposite force directions; the force magnitudes correlated positively. The different regression lines in *Y* panel are due to slightly different angular positions of the handle for each external torque conditions (see the caption to Fig. 3).

NIH-PA Author Manuscript
NIH-PA Author Manuscript
NIH-PA Author Manuscript

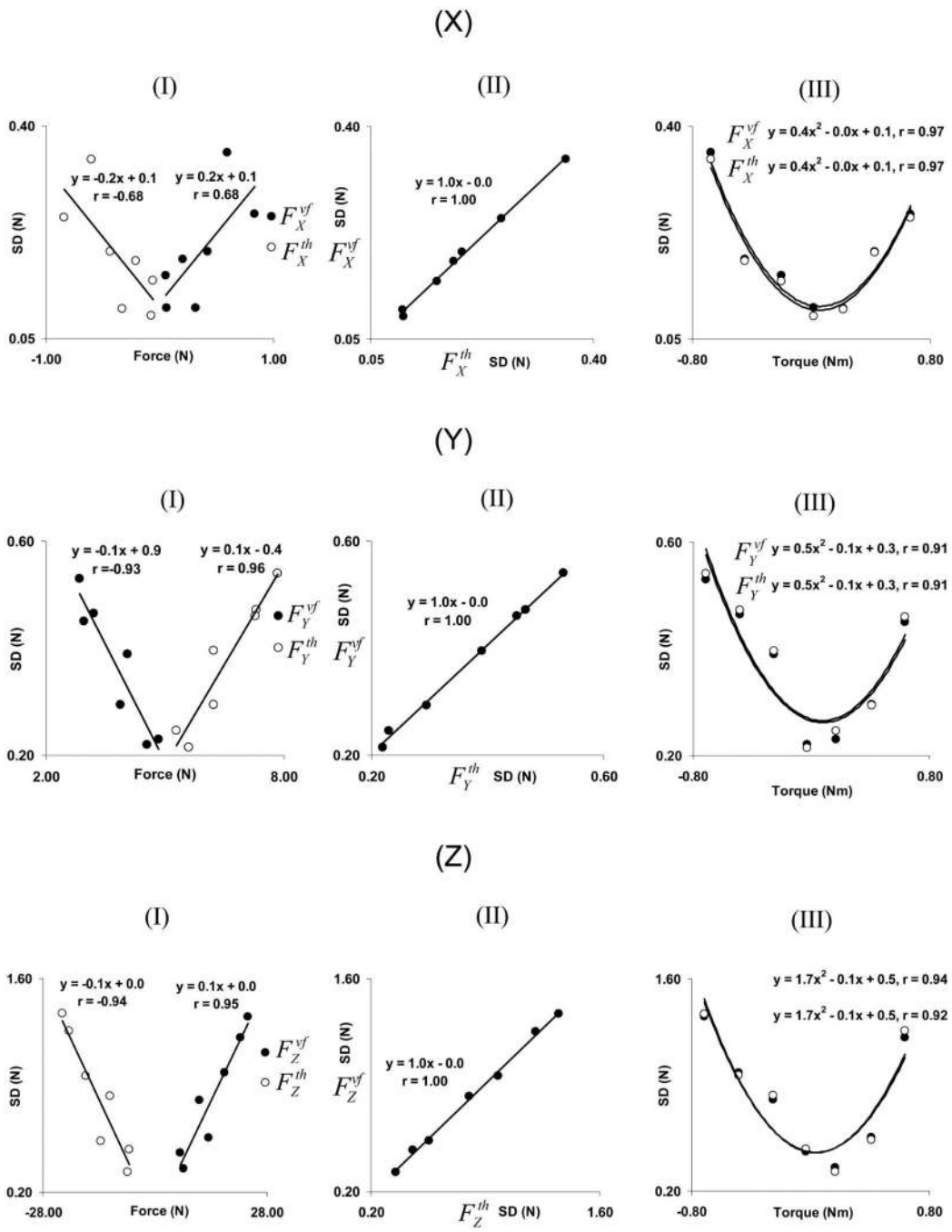

FIG. 5.

SD of the VF and thumb forces. One data point in each figure represents SD over 25 trials for each external condition from a representative subject. (X–I) SD of F_x^{vf} and F_x^{th} vs. the corresponding force magnitudes, (X–II) SD of [F_x^{vf} vs. SD of F_x^{th}, (X–III) F_x^{vf} and F_x^{th} vs. external torque, (Y–I) SD of F_y^{vf} and F_y^{th} vs. the corresponding force magnitude, (Y–II) SD of F_y^{vf} vs. SD of F_y^{th}, (Y–III) F_y^{vf} and F_y^{th} vs. external torque, (Z–I) SDs of F_z^{vf} and F_z^{th} vs. the corresponding force magnitude, (Z–II) SD of F_z^{vf} vs. SD of F_z^{vf}, and (Z–III) F_z^{vf} and F_z^{th} vs. external torque.

NIH-PA Author Manuscript

NIH-PA Author Manuscript

NIH-PA Author Manuscript

TABLE 1

Loadings of principal components ($PC1_X$ and $PC2_X$) for the M_x group

Variable	$PC1_X$	$PC2_X$
$M_x^{vf(y)}$	*1.00*	–0.07
$M_x^{vf(z)}$	*–1.00*	0.04
$M_x^{th(y)}$	*1.00*	–0.07
F_z^{vf}	–0.05	*1.00*
F_z^{th}	0.04	*–1.00*

Data are from the –0.70 Nm external torque condition for a representative subject. The loadings with larger magnitudes are shown in italics.

NIH-PA Author Manuscript

NIH-PA Author Manuscript

NIH-PA Author Manuscript

TABLE 2

Loadings of principal components ($PC1_Y$ and $PC2_Y$) for the M_y group

Variable	$PC1_Y$	$PC2_Y$
$M_y^{vf(z)}$	*1.00*	–0.28
$M_y^{vf(x)}$	*–1.00*	0.16
$M_y^{th(x)}$	*1.00*	–0.18
F_z^{vf}	0.17	*–1.00*
F_z^{th}	–0.16	*1.00*

Data are from the –0.70 Nm external torque condition for a representative subject. The loadings with larger magnitudes are shown in italics.

NIH-PA Author Manuscript

NIH-PA Author Manuscript

NIH-PA Author Manuscript

TABLE 3

Loadings of principal components ($PC1_Z$, $PC2_Z$ and $PC3_Z$) for the M_z group

Variable	$PC1_Z$	$PC2_Z$	$PC3_Z$
m_z^{vf}	–0.01	*0.96*	–0.12
m_z^{th}	–0.38	–0.15	0.93
$m_z^{(C)}$	*0.79*	–0.01	–0.31
$M_x^{vf(x)}$	*–0.94*	–0.02	0.17

Data from the –0.70 Nm external torque condition for a representative subject are shown. The loadings with larger magnitudes are shown in italics. Note that F_x^{vf}, F_y^{vf}, and $M_z^{vf(y)}$ are not included in the table because the loadings were not significant (<0.40) in any of the three PCs.

NIH-PA Author Manuscript

NIH-PA Author Manuscript

NIH-PA Author Manuscript

TABLE 4

Loadings of principal components ($PC1_{3D}$ to $PC3_{3D}$) in all elemental variables

Variable	$PC1_{3D}$	$PC2_{3D}$	$PC3_{3D}$
$M_x^{\mathrm{vf}(y)}$	*0.89*	0.00	–0.27
$M_x^{\mathrm{vf}(z)}$	*–0.92*	0.02	0.26
$M_x^{\mathrm{th}(y)}$	*0.90*	0.03	–0.27
$M_y^{\mathrm{vf}(z)}$	0.01	*–0.99*	0.07
$M_y^{\mathrm{vf}(x)}$	0.00	*0.97*	–0.04
$M_y^{\mathrm{th}(z)}$	–0.02	*–0.99*	0.06
F_z^{vf}	–0.25	–0.10	*0.97*
F_z^{th}	0.26	0.07	*–0.96*

Data are from the –0.70 Nm external torque condition by a representative subject. The loadings with larger magnitudes are shown in italics. Note that m_z^{vf}, m_z^{th}, $m_z^{(\mathrm{C})}$, $M_z^{\mathrm{vf}(x)}$, and $M_z^{\mathrm{vf}(y)}$ are not included in the table because the loadings were not significant (<0.40) in any of the three PCs.